Hindawi
Wireless Communications and Mobile Computing
Volume 2022, Article ID 5747959, 7 pages
https://doi.org/10.1155/2022/5747959

*Research Article*

# Multiband RoF System with Good Transmission Performance Based on Additional SCS

**Anliang Liu and Hongzhi Li**

*School of Information Science and Technology, Dalian Maritime University, Dalian, China*

Correspondence should be addressed to Anliang Liu; alliu@dlmu.edu.cn

Received 16 June 2022; Accepted 8 August 2022; Published 22 August 2022

Academic Editor: Jun Li



A wavelength division multiplexing radio-over-fiber (WDM-RoF) system that can support multiband radio signals based on an additional subcentral station (SCS) is proposed and demonstrated in this paper. The dispersion characteristics of the multiband radio signals over fiber transmission are explored, and we exploit an improved transmission structure consisting of the central station (CS), the SCS, and base stations (BSs) to optimize the antidispersion performance of the proposed RoF system. At the SCS, a dual-drive Mach-Zehnder modulator (MZM) is employed to realize a cost-effective multiband radio signal generation of WDM signals with great spectral flatness, and an optical cross-connect unit is utilized to achieve a flexible distribution of different band radio signals for remote BSs. Based on the additional SCS, we establish a verification WDM-RoF system, which can support reliable transmission of multiband radio signals including 13 GHz, 26 GHz, 39 GHz, and 52 GHz. The WDM signals with each data rate at 2.5 Gbps are successfully transmitted over a 40 km standard single-mode fiber.

## 1. Introduction

Affected by the COVID-19, network office and online education have become the main solutions for people's daily work and learning. The demand of mobile users for high-speed, large-capacity, and reliable communication networks has suddenly increased, and it is in line with the enhanced mobile broadband (eMBB) application scenario in the fifth-generation mobile communication technology (5G) communication systems, which means to provide users with the ultimate high-speed communication experience [1, 2]. Under the current limited spectrum resources, the 3GPP organization for the first time enabled a high-band frequency ranging from 24.25 GHz to 52.6 GHz to achieve a higher data rate transmission in the 5G system [3]. Various countries have carried out a series of studies on the high-band communication systems according to the distribution of their own spectrum resources, as shown in Table 1 specifically [4, 5]. The high-band communication systems are mainly concentrated in several radiofrequency (RF) bands such as 26 GHz, 28 GHz, and 39 GHz. With the increasing demand for data rate, more and more high-band carriers will be developed and utilized in 5G and even future sixth-generation mobile communication technology (6G) communication systems [6, 7]. Therefore, the collaborative communication technology between multiband radio signals is of great significance for large-capacity communication and effective signal coverage, which means that the research on reliable transmission and efficient generation of multiband radio signals is very essential for future mobile communication systems.

The transmission distance of high-band radio carriers is mainly limited by air attenuation, and radio-over-fiber (RoF) technology has become a preferred solution for long-distance and reliable transmission in 5G high-band communication systems [8]. In RoF systems, the generation of high-band radio carriers can be realized in the optical domain, which can effectively simplify the system structure and save implementation costs. The current implementation schemes are mainly based

Table 1: Deployments of 5G high bands.

| Country | Frequency (GHz) |
|---|---|
| China | 24.25~27.5; 37~43.5 |
| USA | 27.5 ~ 28.35; 37~40 |
| Europe | 24.25~27.5 |
| Korea | 26.5 ~ 29.5 |
| Japan | 27.5 ~ 28.28 |

on optical heterodyne, optical nonlinearity, and external modulation methods [9–13]. Among them, the external modulation technology based on the Mach-Zehnder modulator (MZM) has been widely investigated with its great flexibility, high bandwidth, and linearity [14]. Traditional optical carrier suppression modulation can be used to achieve a frequency-doubled electrical signal generation [15]. In reference [16], a W-band millimeter-wave (MMW) signal is generated by a frequency quadrupling technology with one single MZM and a wavelength selective switch (WSS). A 24 GHz microwave signal is obtained by a frequency octupling method based on a dual-polarization quadrature phase shift keying modulator [17]. Moreover, based on a 16-tupling frequency MMW generation scheme without filters, a 160 GHz electrical signal is obtained with two MZMs [18]. Other architectures with more MZMs are proposed to realize a high-band MMW signal generation [19–21]. However, with the increasing number of modulators, the system structure becomes more complex. However, the abovementioned structures mostly carried out the generation of a single RF carrier through a low-frequency local oscillator (LO). As far as we know, few studies focus on how to generate multiple RF carriers at different bands efficiently. In addition, compared with the traditional RoF systems, it becomes more difficult to overcome the fiber dispersion for a high-reliability transmission as the number of high-band signals increases. Therefore, the efficient generation, flexible allocation, and reliable transmission of multiband radio signals in the RoF system is essential for its application in future high-band communication systems.

In this paper, a flexible RoF system based on an additional subcentral station (SCS) that can support multiband radio signals for cooperative communication with great dispersion tolerance is proposed and demonstrated. The different numbers of high-quality optical sidebands is generated by setting appropriate parameters of a dual-arm MZM modulator. We build a verification system with one light source and analyze the influence of the fiber dispersion on the reliability of data transmission at different RF carriers. To achieve the generation and reliable transmission of a large number of multiband radio signals, we establish a wavelength division multiplexing (WDM) RoF system based on the SCS structure, which can transmit several RF signals including 13 GHz, 26 GHz, 39 GHz, and 52 GHz. A centralized multiband RF signal generation structure and an optical cross-connect (OXC) unit are utilized to realize cost-effective generation and flexible allocation of different RF signals. A reliable transmission of 3-channel WDM signals with each data rate at 2.5 Gbps over 40 km optical fiber has been demonstrated by the measured eye diagrams and bit error rate (BER) curves.

## 2. Principle

The principle of optical multiband MMWs generation based on the external MZM is to create new optical harmonics by setting a couple of appropriate parameters of the modulator. Generally, new order sidebands are generated at the central station (CS) with a low frequency LO. At the base stations (BSs), the modulated optical signal can be converted to electrical RF signals at different frequencies after the beat function of the photodetector (PD). The structure diagram of a dual-arm $LiNbO_3$-MZM is shown in Figure 1.

The input optical carrier can be expressed as

$$E_{\text{in}}(t) = E_c e^{j\omega_c t}, \tag{1}$$

where $E_c$ is the amplitude and $\omega_c$ is the angular frequency of the input optical signal. The input signal is equally divided into the upper and lower channels through a Y-shaped waveguide. The phase of optical signals is controlled by the input RF signals and the DC bias voltages in each arm. The recombined signal at the output port can be expressed as

$$E_{\text{out}}(t) = \frac{1}{2} E_{\text{in}} \left[ e^{j(\pi/V_\pi)[V_1(t)+V_{\text{bias1}}]} + e^{j(\pi/V_\pi)[V_2(t)+V_{\text{bias2}}]} \right], \tag{2}$$

where $V_\pi$ is the half-wave voltage of the MZM. $V_1(t)$ and $V_2(t)$ are the RF signals loaded on the upper and lower arms, respectively. $V_{\text{bias1}}$ and $V_{\text{bias2}}$ are the DC bias voltages severally. Normally, the MZM is set to work in push-pull mode, which means $V_1(t) = -V_2(t)$, and they can be described as

$$\begin{aligned} V_1(t) &= V_{\text{RF}} \cos(\omega_{\text{RF}} t), \\ V_2(t) &= V_{\text{RF}} \cos(\omega_{\text{RF}} t + \Delta\theta), \end{aligned} \tag{3}$$

where $V_{\text{RF}}$ and $\omega_{\text{RF}}$ are the amplitude and angular frequency term of the RF signal, respectively. Where $\Delta\theta = (2k+1)\pi$, it is the phase difference between the two modulated RF signals. Then, equation (2) can be simplified by the Bessel function expansion as

$$E_{\text{out}}(t) == \frac{1}{2} E_{\text{in}} e^{j(V_a/2)} \left\{ \sum_{n=-\infty}^{+\infty} J_n(m) e^{jn(\omega_{\text{RF}} t + ((\Delta\theta+\pi)/2))} \cos\left(\frac{\Delta\varphi}{2} + n\frac{\Delta\theta}{2}\right) \right\}, \tag{4}$$

where $m = \pi V_{\text{RF}}/V_\pi$ is the modulation index, $V_a = \pi(V_{\text{bias1}} + V_{\text{bias2}})/V_\pi$, $\Delta\varphi = \pi(V_{\text{bias1}} - V_{\text{bias2}})/V_\pi$, and $J_n(\bullet)$ is the first kind Bessel function of $n$th order. It can be seen that the intensity of different order optical sidebands can be controlled by the modulation depth $m$, the phase difference of the modulation signal, and the magnitude of the bias voltage. For example, when $m = 1.84$, $\Delta\varphi = 1.76V_\pi$, and $\Delta\theta = \pi$, the amplitudes of different order sidebands $|E_0| \approx |E_{\pm1}| \approx |E_{\pm2}|$, which means a five-line comb with a great flatness can be acquired. By detecting the generated optical comb lines, the electrical RF signals at different bands can be obtained.

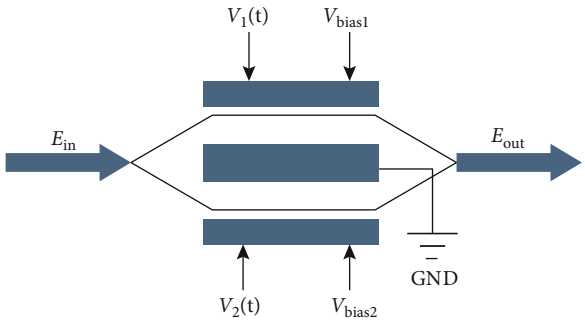


Figure 1: Typical structure of $LiNbO_3$-MZM.

Therefore, with the above structure, only one LO has been utilized to achieve a centralized generation of multiple RF signals, which can effectively reduce the cost of multiband radio signal generation.

## 3. Simulation Results and Discussion

*3.1. Multiband RoF System Based on CS-BS Structure.* According to the principle of multiband radio signal generation with the MZM modulator mentioned in the previous section, we build a multiband RoF verification system based on the traditional CS-BS structure to analyze its transmission characteristics. The system architecture is shown in Figure 2.

At the CS, the laser diode (LD) with a wavelength of 1550 nm is injected to a dual-arm MZM after the polarization controller (PC). The optical carrier is modulated by a RF signal that consists of a 13 GHz LO and a 2.5 Gbps baseband data signal. The half-wave voltage $V_\pi$ of the modulator is 4 V. Under the push-pull operation mode, to acquire a five optical comb-line, the bias voltage of MZM is set to $V_{bias} = V_\pi = 4$ V and the amplitude of the mixed RF signal is set to 2.34 V to set the modulation index $m$ to 1.84. The optical spectrum of the MZM output optical is shown in Figure 2(a). The frequency of the central optical carrier is 193.1 THz, and the comb line spacing is 13 GHz, which has a great flatness of 0.35 dB, and an unwanted-mode suppression ratio of 15 dB. The modulated signal is amplified by an erbium-doped fiber amplifier (EDFA) with a gain of 20 dB and then transmitted to the receiver over a standard single-mode fiber (SSMF).

At the BS, a PD is used to convert the optical signal to multiband radio signals. The spectrum of the detected electrical signal is shown in Figure 2(b). It can be seen that multiple signals at different frequencies including 13 GHz, 26 GHz, 39 GHz, and 52 GHz are achieved. And they can be selected and transmitted to mobile users by the RF antenna. In order to analyze the transmission characteristics of these RF signals over the fiber system, a tunable band-pass filter (BPF) and different LOs (including 13 GHz, 26 GHz, 39 GHz, and 52GHz) are employed to downconvert each received RF signal. The original baseband data signal can be recovered from different frequency carriers after a low-pass filter (LPF), and the eye diagrams can be measured by an oscilloscope. By changing the fiber length, the bit error rate curves for different RF signals are measured and as shown in Figure 3. Due to the influence of the fiber dispersion, the reliability of data signals with lower-frequency carriers is better than the data with higher-frequency carriers. Moreover, the original baseband data signal is modulated to each new generated optical carrier, the periodic fading effect has a much more serious impact on the multiband RoF system.

The power of the received RF signals at 13 GHz, 26 GHz, and 39 GHz is influenced by the transmission length. As the frequencies of RF signals increase, the power fading points appear more frequently. For example, when the transmission distance is 12.5 km, the data transmission performance on the 13 GHz carrier frequency decreases significantly, while the data transmission quality on other frequency carriers is better. Particularly, the 52 GHz RF carrier signal can be immune to the power fading effect because it comes from the ±2nd-order sidebands. With the increasing number of different frequency carries, it becomes more difficult to select a suitable optical fiber transmission distance to avoid the power fading points and achieve reliable signals transmission. In order to suppress the influence of chromatic dispersion on system reliability, the amount of frequency spectrum entering the beat frequency of the photodetector should be decreased.

*3.2. Multiband WDM-RoF System Based on Additional SCS.* A multiband WDM-RoF system based on the CS-SCS-BS structure is proposed to improve the transmission performance of different RF carriers. The proposed system structure is shown in Figure 4.

Baseband data signals are utilized between the CS and SCS to alleviate the serious impact of fiber dispersion on link reliability. Multichannel downstream signals are transmitted to the remote SCS through a single optical fiber by wavelength division multiplexing and then centrally modulated by the MZM-based multiband RF signals generation structure mentioned above. The modulated optical signals consist of multiorder spectral components. An additional OXC unit is employed to realize a flexible separation of the downstream signals at different frequencies for their respective BSs. Since the SCS is close to the BS sides, the dispersion effect can be ignored. Thus, the additional SCS can greatly improve the dispersion resistance and flexibility of the proposed multiband WDM-RoF system.

A verification structure of the multiband WDM-RoF system is shown in Figure 5. At the CS, $3 \times 2.5$ Gbps baseband data are modulated to the optical TXs (transmitters) with different central frequencies of $f_1 = 1552.52$ nm, $f_2 = 1551.72$ nm, and $f_3 = 1550.92$ nm, respectively. The modulated optical signals are multiplexed by a WDM multiplexer and then amplified by an EDFA. The fiber length between the CS and SCS is set to 40 km. The downstream signals are centrally modulated by a 13 GHz LO to realize 5 optical lines generation for each optical carrier. The output optical spectra are shown in Figure 5(a). The flatness of the new generated optical lines is less than 0.5 dB, and the unwanted-mode suppression ratio is more than 15 dB for each optical carrier.

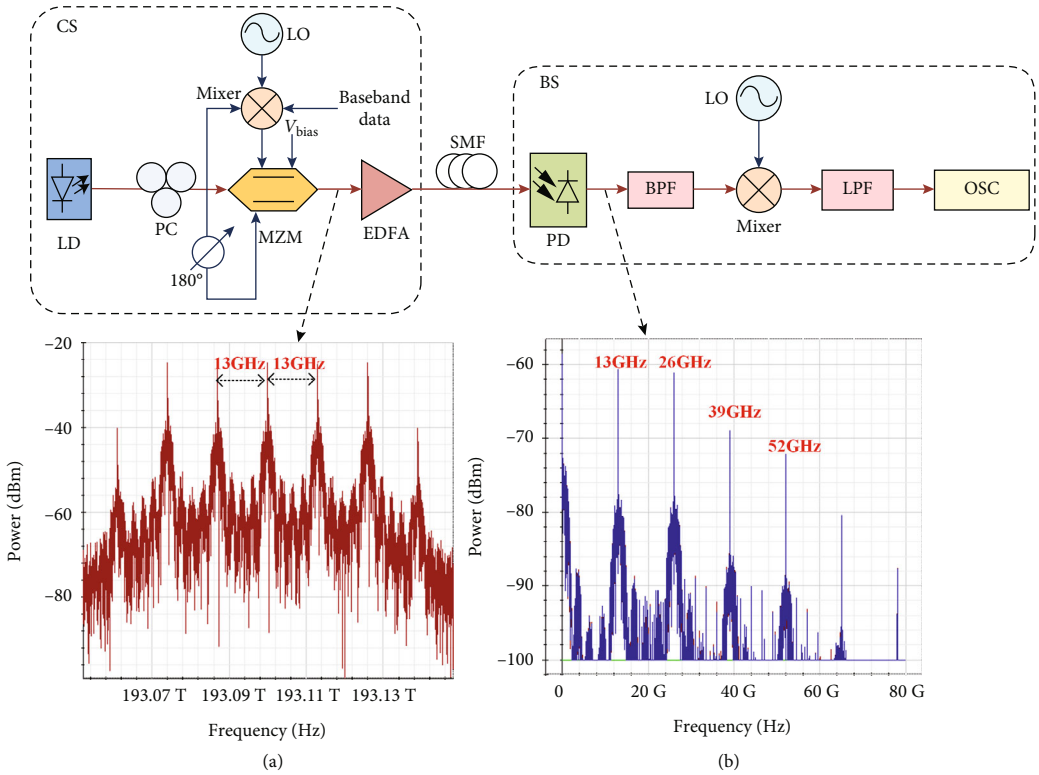


Figure 2: Schematic setup of multiband RoF system. (a) Output optical spectra after MZM. (b) Detected RF signal spectra after PD.

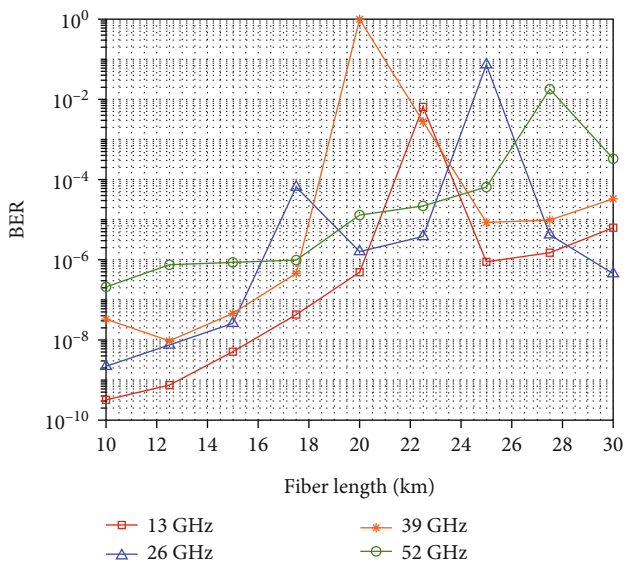


Figure 3: BER curves versus fiber lengths for different RF signals.

An OXC unit consisting of a WSS with a minimum slice of 12.5GHz and two optical couplers (OCs) is employed to implement an allocation for different RF signals. For example, if a 26 GHz RF signal needs to be transmitted to the BS1 through the optical carrier at $f_1$, the WSS slice number of output port 1 should be set to 141~142 as a band pass filter which central frequency is 193.0875 THz and the bandwidth is from 193.075 THz to 193.1 THz and the slice number of output port 2 is set to 143~144 which central frequency is 193.0875 THz and the bandwidth is from 193.1 THz to 193.125 THz. The new generated ±1st-order sidebands will be filtered out and then recombined by an OC. The output spectra after WSS is shown in Figure 5(b). At the BS1, a PD is used to convert the optical signal to the 26 GHz RF signal. In order to analyze the reliability of system transmission, a LO is employed to recovered the original baseband data and measured by a BERT (bit error rate tester).

By changing the parameters of the WSS at the SCS, several specified RF signals can be sent to BS1. The measured BER curves for different RF signals are shown in Figure 6. It can be found that the BER of 13 GHz, 26 GHz, 39 GHz, and 52 GHz signals can reach $3.8 \times 10^{-3}$ when the received signal power is about −25 dBm. In particular, the BER of 52 GHz signal can be as low as $10^{-6}$ due to the width of the WSS slice and the data rate of the baseband signal. The RF signals over different optical carriers can also be distributed to each remote BS. The BER curves of 26 GHz RF signal over different wavelengths are shown in Figure 7. It can be seen that the optical receiver sensitivity is approximately −25 dBm with the BER $< 3.8 \times 10^{-3}$. On the basis of the proposed multiband RF signals generator and the optical wavelength switch unit at the SCS, more RF signals at different frequencies can be obtained and delivered to the required BSs. Furthermore, the multiband radio signal generation structure

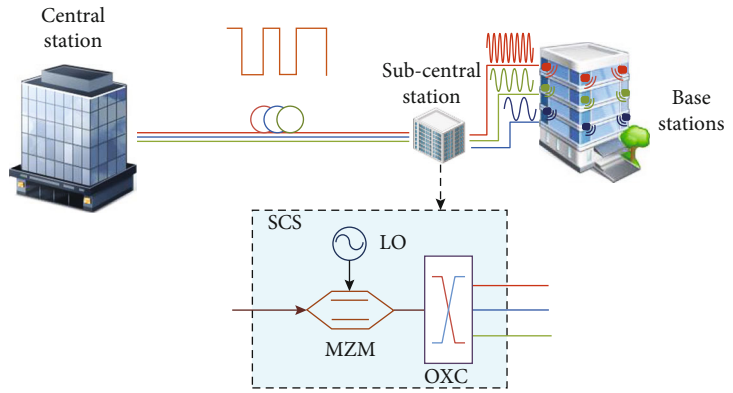


Figure 4: Architecture of the proposed multiband WDM-RoF system.

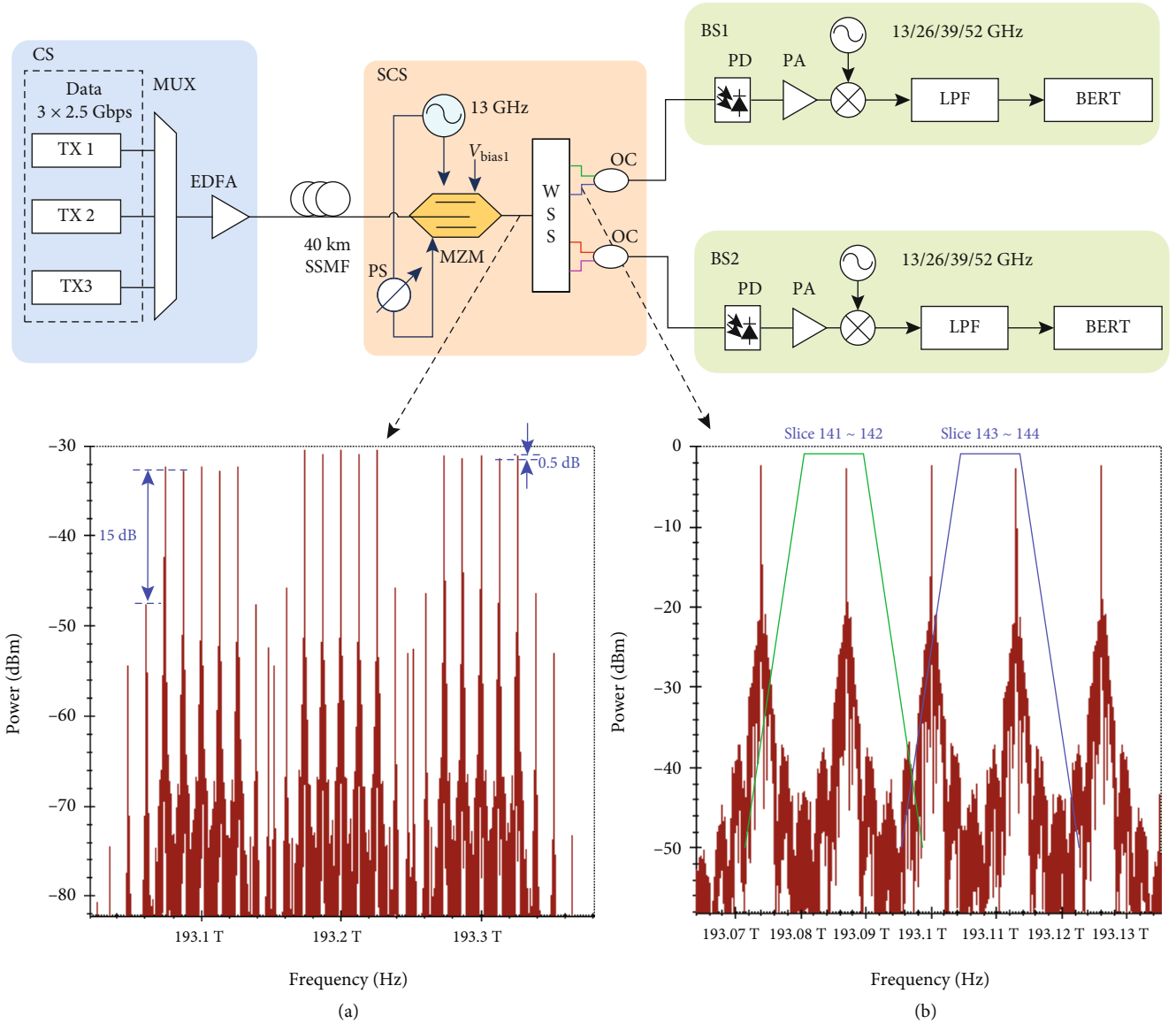


Figure 5: Mutiband WDM-RoF verification system based on the additional SCS. (a) Output optical spectra of the MZM. (b) Spectra after WSS at the SCS.

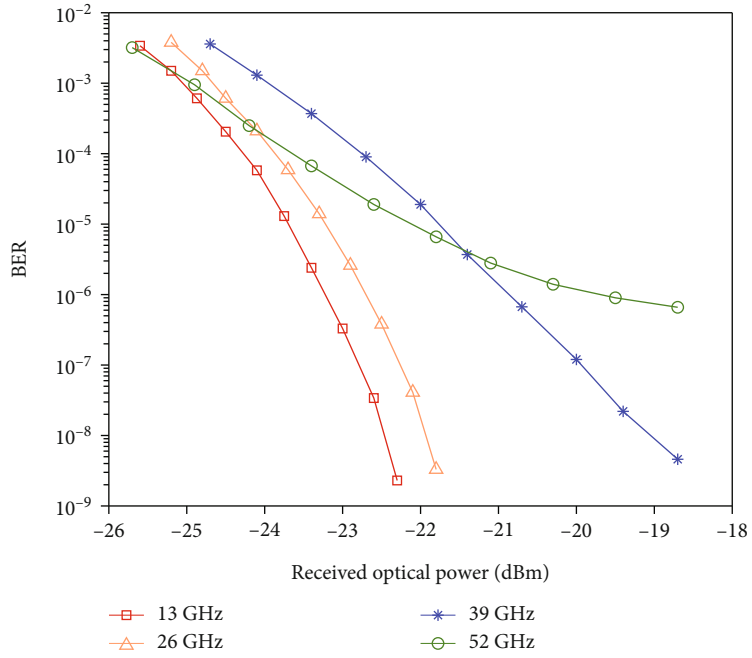


Figure 6: BER curves for multiband radio signals.

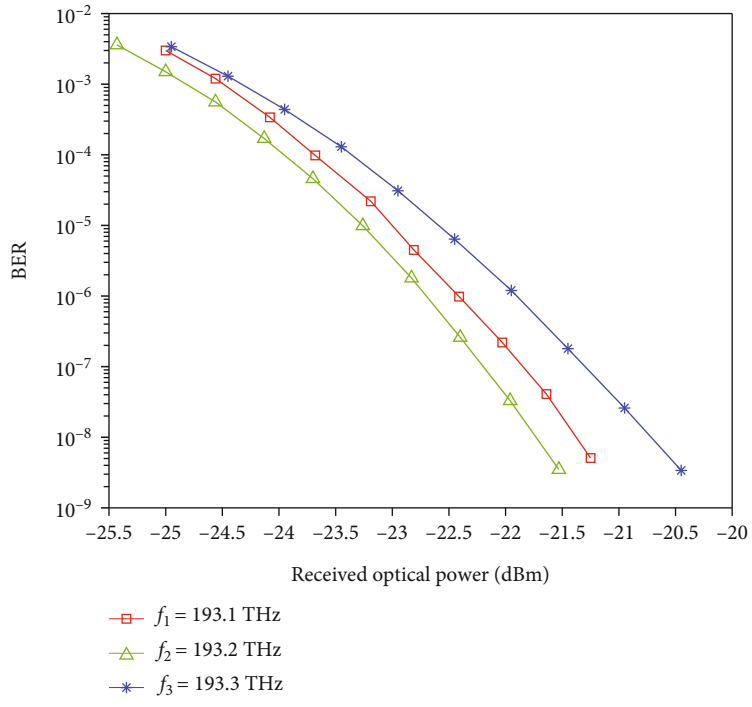


Figure 7: BER curves of 26 GHz RF signal over different optical carriers.

can be further expanded if the phase noise of the adjacent optical carriers be controlled effectively.

## 4. Conclusions

In this paper, a WDM-RoF system with multiband radio signals based on the CS-SCS-BS structure is proposed with a great dispersion tolerance and flexibility. On the basis of the external MZM, a centralized multiband RF signals generation structure with great flatness for the WDM signal is realized at the SCS, which can not only improve the capacity of the RoF system but also effectively eliminate the dispersion influence on the reliability of the multiband communication system. Moreover, with the use of the WSS and OCs

unit, the system can achieve a flexible allocation of different RF signals to different BSs. Finally, an experimental verification RoF system with three channels WDM signal at 2.5 Gbps which can support multiband radio signals including 13 GHz, 26 GHz, 39 GHz, and 52 GHz over a 40 km SSMF is demonstrated and its communication reliability is achieved. The proposed multiband WDM-RoF system is of great significance in future cooperative and high-band communication systems.

## Data Availability

The data that support the findings of this study are available from the corresponding author upon reasonable request.

## Conflicts of Interest

The authors declare that they have no competing interests.

## Acknowledgments

This work is supported in part by the China Postdoctoral Science Foundation under Grant 2019M651095 and the Fundamental Research Funds for the Central Universities under Grant 3132019348.

## References

[1] P. T. Dat, A. Kanno, N. Yamamoto, and T. Kawanishi, "Seamless convergence of fiber and wireless systems for 5G and beyond networks," *Journal of Lightwave Technology*, vol. 37, no. 2, pp. 592–605, 2019.

[2] R. Li, Z. Zhao, X. Zhou et al., "Intelligent 5G: when cellular networks meet artificial intelligence," *IEEE Wireless Communications*, vol. 24, no. 5, pp. 175–183, 2017.

[3] J. Lee, E. Tejedor, K. Ranta-aho et al., "Spectrum for 5G: global status, challenges, and enabling technologies," *IEEE Communications Magazine*, vol. 56, no. 3, pp. 12–18, 2018.

[4] M. J. Marcus, "ITU WRC-19 Spectrum Policy Results," *IEEE Wireless Communications*, vol. 26, no. 6, pp. 4-5, 2019.

[5] Huawei, *5G Spectrum–Public Policy Position*, White paper, 2016.

[6] L. Zhang, M. Xiao, G. Wu, M. Alam, Y. C. Liang, and S. Li, "A survey of advanced techniques for spectrum sharing in 5G networks," *IEEE Wireless Communications*, vol. 24, no. 5, pp. 44–51, 2017.

[7] W. Saad, M. Bennis, and M. Chen, "A vision of 6G wireless systems: applications, trends, technologies, and open research problems," *IEEE Network*, vol. 34, pp. 134–142, 2019.

[8] J. Yao, "Microwave photonics," *Journal of Lightwave Technology*, vol. 27, no. 3, pp. 314–335, 2009.

[9] H. J. Kbashi, V. Sharma, and S. Sergeyev, "Phase-stable millimeter-wave generation using switchable dual-wavelength fiber laser," *Optics and Lasers in Engineering*, vol. 137, article 106390, 2021.

[10] U. Gliese, T. N. Nielsen, S. Nørskov, and K. E. Stubkjaer, "Multifunctional fiber-optic microwave links based on remote heterodyne detection," *IEEE Transactions on Microwave Theory and Techniques*, vol. 46, no. 5, pp. 458–468, 1998.

[11] R. Pant, D. Marpaung, I. V. Kabakova, B. Morrison, C. G. Poulton, and B. J. Eggleton, "On-chip stimulated Brillouin scattering for microwave signal processing and generation," *Laser & Photonics Reviews*, vol. 8, no. 5, pp. 653–666, 2014.

[12] W. Xu, X. Gao, M. Zhao, M. Xie, and S. Huang, "Full duplex radio over fiber system with frequency quadrupled millimeter-wave signal generation based on polarization multiplexing," *Optics and Laser Technology*, vol. 103, pp. 267–271, 2018.

[13] J. Tang, J. Sun, L. Zhao, T. Chen, T. Huang, and Y. Zhou, "Tunable multiwavelength generation based on Brillouin-erbium comb fiber laser assisted by multiple four-wave mixing processes," *Optics express*, vol. 19, no. 15, pp. 14682–14689, 2011.

[14] J. Ma, J. Yu, C. Yu, X. Zhang, j. Zeng, and L. Chen, "Fiber dispersion influence on transmission of the optical millimeter-waves generated using LN-MZM intensity modulation," *Journal of Lightwave Technology*, vol. 25, no. 11, pp. 3244–3256, 2007.

[15] J. Yu, Z. Jia, L. Yi, Y. Su, G. K. Chang, and T. Wang, "Optical millimeter-wave generation or up-conversion using external modulators," *IEEE Photonics Technology Letters*, vol. 18, pp. 265–267, 2006.

[16] L. Chen, R. Deng, J. He, Q. Chen, Y. Liu, and C. Xiang, "W-band vector signal generation by photonic frequency quadrupling and balanced pre-coding," *IEEE Photonics Technology Letters*, vol. 28, no. 17, pp. 1807–1810, 2016.

[17] Y. Gao, A. Wen, W. Jiang, D. Liang, W. Liu, and S. Xiang, "Photonic microwave generation with frequency octupling based on a DP-QPSK modulator," *IEEE Photonics Technology Letters*, vol. 27, no. 21, pp. 2260–2263, 2015.

[18] D. Wang, X. Tang, L. Xi, X. Zhang, and Y. Fan, "A filterless scheme of generating frequency 16-tupling millimeter-wave based on only two MZMs," *Optics and Laser Technology*, vol. 116, pp. 7–12, 2019.

[19] Y. Wang, L. Pei, J. Li, and Y. Li, "Full-duplex radio-over-fiber system with tunable millimeter-wave signal generation and wavelength reuse for upstream signal," *Applied Optics*, vol. 56, no. 17, pp. 4982–4989, 2017.

[20] Y. Chen, A. Wen, J. Guo, L. Shang, and Y. Wang, "A novel optical mm-wave generation scheme based on three parallel Mach-Zehnder modulators," *Optics Communications*, vol. 284, no. 5, pp. 1159–1169, 2011.

[21] H. Chen, T. Ning, J. Li et al., "Optical millimeter-wave generation with tunable multiplication factors and reduced power fluctuation by using cascaded modulators," *Optics and Laser Technology*, vol. 103, pp. 206–211, 2018.